doi: 10.22564/brjg.v8i1-2.1085

Revista Brasileira de Geofísica; 1990, Vol. 8 (1), 23-34

THE BROADBAND ELECTROSTATIC NOISE IN THE EARTH'S MAGNETOTAIL*

L. GOMBEROFF[1]

A brief history of the broadband electrostatic noise in the Earth's magnetotail is presented. The most important aspects which led to the present understanding of these emissions in terms of a combination of several instabilities are discussed. An analytical approach to the ion-acoustic and ion-ion acoustic instabilities is given. It is shown, in particular, that the ion-ion acoustic instability is a resonant kinetic type instability. Although the broadband electrostatic noise seems to be fairly well understood, some problems still unsolved are briefly discussed.

RUIDO ELETROSTÁTICO DE BANDA LARGA NA MAGNETOCAUDA DA TERRA – Apresenta-se um breve histórico do ruído eletrostático de banda larga na magnetocauda da Terra. São discutidos os aspectos mais importantes que levaram à atual compreensão dessas emissões em termos de uma combinação de várias instabilidades. É feito um tratamento analítico das instabilidades ion-acústica e ion-ion acústica. Mostra-se que a instabilidade ion-ion acústica é do tipo cinético ressonante. Embora o ruído eletrostático de banda ampla parece ser bem compreendido, ainda existem alguns problemas não resolvidos, que são aqui discutidos.

1. INTRODUCTION

The purpose of this paper is twofold. First, to make a review of the main development which led to our present understanding of the broadband electrostatic noise (BEN) observed in the plasma sheet boundary layer (PSBL) and, second, to make a detailed analytical study of the ion-ion acoustic instability, which is believed to be one of several instabilities involved in the generation of the BEN.

The ion-ion acoustic instability has been the subject of several studies (Forslund & Shonk, 1970; Grabbe & Eastman, 1984; Omidi, 1985; Akimoto & Omidi, 1986; Dusenbury & Lyons, 1985; Gary & Omidi, 1987). Most of these studies are based on numerical solutions of the exact dispersion relation, and, although the main properties of the ion-ion acoustic instability are fairly well understood, there are still some questions concerning its nature. Thus while some authors claim that it is a fluid like instability (Omidi & Akimoto, 1988), others think that it is a resonant kinetic like instability (Dusenbery, 1988).

The analytical method developed here leads to a system of coupled equations, which describes both the ion-acoustic and the ion-ion acoustic instabilities. A priori, it is difficult to separate the effects leading to each one of the instabilities. However, when the equations are complemented with the marginal instability condition, the effects leading to each instability can be clearly discerned. The method shows unambigously that the ion-ion acoustic instability is due to Landau kinetic effects.

The paper is organized in the following way: In Section II a brief history of the BEN is present. In Section III an analytical approach to ion beam instabilities is developed. In Section IV the conclusions are summarized and discussed.

II.1 HISTORICAL REVIEW

In Fig. 1 we show a very schematic picture of the magnetosphere. The region of interest is the PSBL, which is the layer that separates the northern and southern lobe regions from the central plasma sheet region.

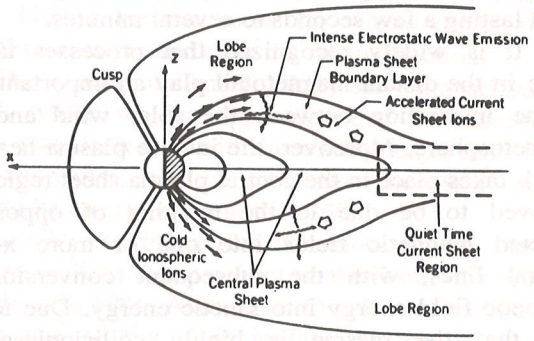

Figure 1. Schematic cross section of the earth's magnetosphere illustrating the generation region of the BEN. (Adapted from Dusenbury & Lyons, 1985).

Scarf et al. (1974) and Gurnett et al. (1976) analysing data from IMP 7 and IMP 8 satellites respectively, discovered strong broadband electrostatic

[1] Universidad de Chile, Facultad de Ciencias, Departamento de Fisica, Casilla 653, Santiago, Chile.

* Invited review presented at the I Latin-American Conference on Space Geophysics, Águas de Lindóia, SP, November 1989.

noise when the satellites crossed from the southern lobe to the northern lobe. These waves have a brodband frequency structure with frequencies ranging from 10 Hz to about 10 kHz. They are most intense and frequent in the PSBL but they have also been observed in the lobe regions and in the central plasma sheet region.

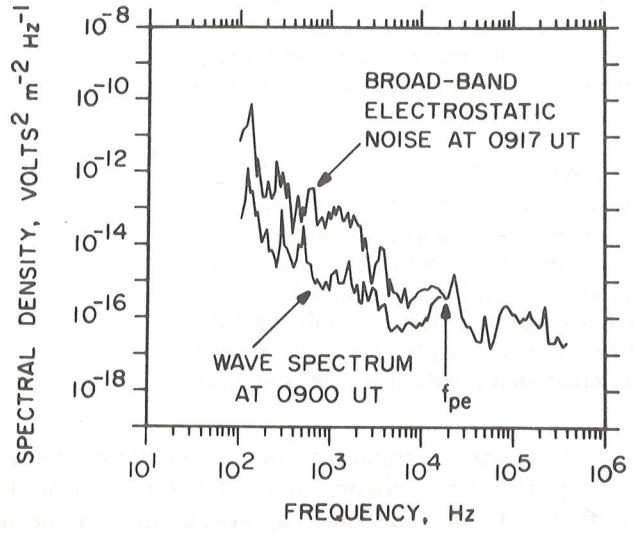

Figure 2. Spectral density vs. frequency spectrum of the BEN for two positions of the satellite. (Adapted from Grabbe & Eastman, 1984).

In Fig. 2, we show the frequency spectrum of the BEN as a function of the spectral density when the satellite was in the southern lobe region (lower curve) and at a later time when it was in the PSBL. The spectrum has a typical V - shape consisting of many burst lasting a few seconds to several minutes.

It is widely recognized that processes taking place in the distant magnetotail play an important role in the interaction between the solar wind and the magnetosphere. Moreover, the intense plasma heating, which takes place in the central plasma sheet region, is believed to be due to the merging of oppositely directed magnetic fields into one or more x-type neutral lines, with the subsequent conversion of magnetic field energy into kinetic energy. Due to the fact that the plasma is highly collisionless, an anomalous resistivity mechanism is required to explain these processes. It is believed that the BEN can play an important role in providing this anomalous resitivity mechanism.

The first attempts to explain the BEN go back to 1977, when Ashour-Abdalla & Thorne proposed an n + 1/2 electrostatic ion-cyclotron harmonic instability as the basic mechanism for the BEN. This instability is generated by a loss cone distribution function. However the instability is quenched when the electron temperature is of the order of and larger than 10 eV and, as we shall see, in the BEN the electron temperature ranges between 200 eV and 500 eV. Thus, this instability cannot generate the BEN.

A year later, Huba et al. (1978), proposed the lower hybrid drift instability as the basic mechanism for the BEN. This instability is generated by density gradients and has an upper frequency cutoff which lies well within the BEN. Therefore, this instability cannot explain the BEN either, or at least, it cannot be responsible for all the waves in the BEN.

Later analysis on ISEE 1 satellite data showed the presence of energetic ion beams in the PSBL. The beams tend to fall into two classes. The first class consists of single beams propagating towards the Earth along the magnetic field lines with velocities ranging from 10^3 up to 1.8 x 10^3 km/s. The second class beams consists of counterstreaming beams propagating towards the Earth and away from the Earth with velocities ranging from 700 up to 1500 km/s.

The plasma composition in the PSBL is as follows:

1. Energetic ion beams with energies ranging from 1 to more than 40 keV, and densities between 0.1 and 0.8 n_o, where n_o is the total electron density.
2. Low energy ions with temperatures ranging between 50-100 eV and densities between 0.1 and 0.8 n_o.
3. High temperature electrons with temperatures between 200-500 eV and densities between 0.5 up to 1.0 n_o. When the hot electron density is less than n_o, a cold electron component seems to be present – most probably of ionospheric origin – and, as we shall see, it may play an important role in the generation of the BEN.

II.2 ATTEMPTS AT EXPLAINING THE BEN BY ION BEAM INSTABILITIES

The presence of ion beams in the PSBL led Grabbe & Eastman (1984) to assume that the BEN could be due to ion-beam instabilities. To this end, they used the dispersion relation for electrostatic waves in a homogeneous plasma in the presence of an external magnetic field:

$$k^2 + 2\pi \sum_{\alpha} \sum_{n=-\infty}^{\infty} \frac{w^2_{p\alpha}}{w^2} \int_{-\infty}^{\infty} d V_{/\!/} \int^{\infty} 2 V_{\perp} J_n^2 (\lambda_\alpha) \mid n \Omega_\alpha^2 \frac{\partial f_{o\alpha}}{\partial V_{\perp}^2}$$

$$+ k_{/\!/} V_{/\!/} (\Omega_\alpha + k_{/\!/} V_{/\!/}) \frac{\partial f_{o\alpha}}{\partial v_{/\!/}} \mid dV_{\perp} \; / \; (w - n \Omega_\alpha + k_{/\!/} V_{/\!/}) \qquad (1)$$

where k is the wavenumber, the sum over α is over all plasma components, $w_{p\alpha}$ is the plasma frequency of species α, J_n is the Bessel function of order n, Ω_α is the gyrofrequency of species α and $k_{/\!/}$ is the component of the wave vector along the magnetic field.

Considering Maxwellian distribution functions for the hot electrons and the low energy ion-core, and a drifting Maxwellian for the ion-beam, Grabbe & Eastman (1984) obtained the following dispersion relation:

$$1 + \frac{2w_{pe}^2}{k^2 \alpha_e^2} \{1 + e^{-k^2 \alpha_e^2/2\Omega_e^2} \frac{w}{k_{/\!/} \alpha_e} \sum_n I_n (\frac{k^2 \alpha^2}{2 \Omega_e^2}) \cdot$$

$$\cdot Z (\frac{w - m \Omega_e}{k_{/\!/} \alpha_e})\} - \frac{w_{pi}^2}{k^2 \alpha_i^2} Z' (\frac{w}{k \alpha_i}) + \frac{w_{pb}^2}{k^2 \alpha_b^2} \cdot$$

$$\cdot Z' (\frac{w - k_{/\!/} V}{k_{/\!/} \alpha_b}) = 0 \qquad (2)$$

where Z is the plasma dispersion function of Fried & Conte (1961), Z' in the last two terms is the first derivative of the plasma dispersion function, the I_n are the modified Bessel functions, and α_e with l = e, i, b the thermal velocities of the electrons ion-core and ion-beam respectively.

The magnetic effects on the ions have been neglected since Ω_i is much smaller than the frequencies in the BEN. However for the electrons, magnetic effects cannot be neglected because Ω_e lies within the BEN.

From eq. (2), Grabbe & Eastman (1984) calculated the growth rate of the waves, which result is shown in Fig. 3, where the growth rate (normalized to the electron plasma frequency) versus the real frequency which is also normalized to the electron plasma frequency, is shown for various propagation angles. The fastest growing waves occur for parallel propagation, and then, there is a steady decrease of the maximum growth rate for larger and larger angles. The unstable frequency range extends from about 10^{-3} up to 10^{-1} w_{pe}, so that there is a broadband frequency spectrum like the BEN.

There are, however, two major shortcomings in the Grabbe and Eastman's model. First, the high frequency cutoff in the BEN goes up to and sometimes beyond w_{pe}, and second, already Gurnett et al. (1976) had observed that the fastest growing waves propagate in a direction perpendicular to the magnetic field (within observational errors of about 20°). Grabbe & Eastman (1984) attributed the differences to wave propagation effects.

However, Omidi (1985) showed that:

1. Grabbe & Eastman (1984) made a mistake in the derivation of the dispersion relation.
2. The magnetic field has no influence on the BEN.
3. The fastest growing waves propagate in a direction of 75° with respect to the magnetic field, in a very good agreement with the observations.

The mistake made by Grabbe & Eastman (1984) lies in the argument of the last function in eq. (2), where they wrote $k_{/\!/}$ instead of k. However, as for parallel propagating waves $k_{/\!/} = k$, the results of Omidi (1985) are the same for waves propagating parallel or almost parallel to the beam direction.

The results of Omidi (1985) are summarized in Fig. 4, where we can appreciate that the maximum growth rate decreases with increasing angle until $\theta = 60°$. Thereafter, the growth rate increases again reaching its largest value at $\theta = 75°$.

Just by looking at the behaviour of the growth rate, one realizes that it cannot be the result of just one instability. In 1986, Akimoto & Omidi showed that the growth rate of Fig. 4 is in fact the results of two instabilities. The instability which peaks at 0° corresponds to the well known ion-acoustic instability and it is due to the relative drift between the electrons and the ion background. The other instability peaks at an angle with the beam direction, and it is due to the relative drift between the ion-core and the ion-beam. The latter instability is called the ion-ion acoustic instability.

In 1986, Cattel & Mozer showed that the peak in wave power spectrum occurs near the lower hybrid instability with a steady decrease in wave power up to

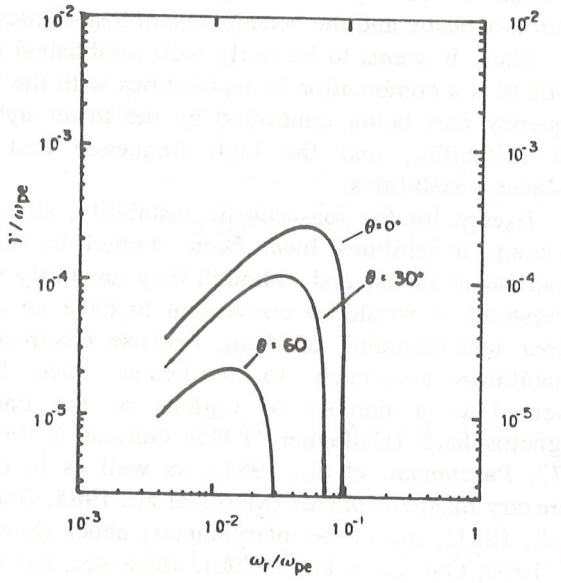

Figure 3. Growth rate vs. frequency both normalized to w_{pe}, as obtained by Grabbe & Eastman (1984).

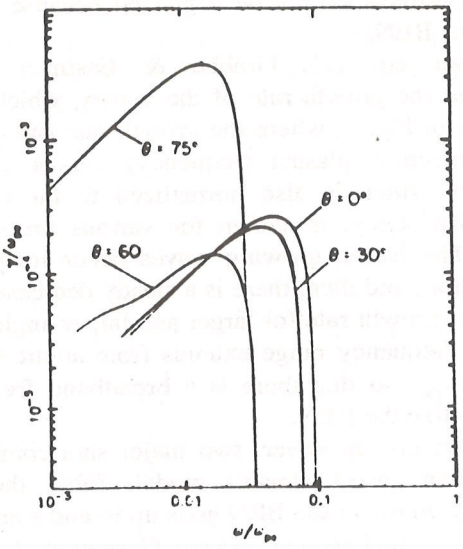

Figure 4. Growth rate vs. frequency both normalized to w_{pe} as obtained by Omidi (1985).

and beyond the electron plasma frequency. This fact led them to suggest that the BEN is a combination of instabilities with the lower hybrid drift instability (first proposed by Huba et al., 1978) being responsible for the low frequency part of the BEN and the ion-beam instabilities (first proposed by Grabbe & Eastman, 1984) being responsible for the high frequency part of the BEN.

Shortly after that, Cattel et al. (1986) discovered strong density and magnetic field gradients in the PSBL giving strong support to the suggestion of Cattel & Mozer (1986).

In 1985, Etcheto & Saint-Marc discovered that when the hot electron density in the PSBL is less than one, there is a cold electron component probably of ionospheric origin. Before this discovery, Grabbe (1985) trying to find a mechanism to enhance the high frequency cut-off of the ion-beam instabilities, realized that the addition of an even very small amount of cold electrons can largely enhance the high frequency cutoff.

In Fig. 5 the results found by Grabbe (1987) are summarized. The plasma model is the same one considered by Grabbe & Eastman (1984) with a minority cold electron component of about 1% of the total electron density. As it can be seen, even such small amount of cold electrons almost doubles the high frequency cutoff. The maximum growth rate of the ion-acoustic instability is also largely increased. Without cold electrons, the largest growth rate is of the order of 2×10^{-4} (see Fig. 4) while with cold electrons the order is of 7×10^{-3}. There is no effect of the cold electrons on the ion-ion acoustic instability. However, if the cold electron density is increased, then there is an increasing stabilization of the ion-ion acoustic instability. For a 10% amount of cold electrons, the high frequency cutoff reaches a value of about 0.5 w_{pe}. An additional increase of cold electrons stabilizes the ion-ion acoustic mode.

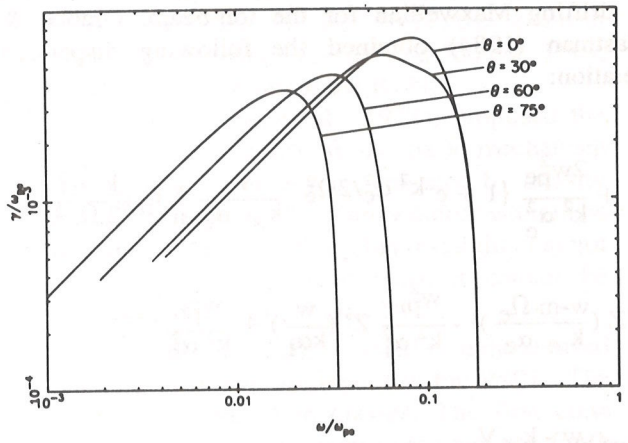

Figure 5. Growth rate vs. frequency both normalized to w_{pe} for on $\eta = 0.01$ concentration of cold electrons.

In 1987, Schriver & Ashour-Abdalla showed that the addition of cold electrons introduces new instabilities into de system. The new instabilities are due to the relative drift between the cold electrons and the ion beam. They receive different names depending on whether the new instabilities are fluid type or kinetic type. In the first case, the instability is the Buneman instabilitiy and in the second case, the electron-acoustic and the beam resonant instabilities.

Thus, it seems to be fairly well established that the BEN is a combination of instabilities with the low frequency part being controlled by the lower hybrid drift instability, and the high frequency part by ion-beam instabilities.

Except for the ion-acoustic instability, all other ion-beam instabilities have been studied by using numerical methods, and although they are fairly well understood, it would be convenient to have an even deeper understanding of them, because electrostatic instabilities associated to ion-beams have been observed in a number of regions of the Earth's magnetosphere (Gallagher, 1985; Gurnett & Frank, 1977; Paschmann et al., 1982), as well as in other planetary magnetospheres (Moses et al., 1985; Gurnett et al., 1981), and in the interplanetary shock (Scarf et al., 1970; Gurnett et al., 1979b). Moreover, the BEN itself has also been observed in the Earth's foreshock (Anderson et al., 1981; Formisano & Torbert, 1982; Gresillon et al., 1975; Paschman et al., 1982; Thomsen, 1985), interplanetary shock (Kennel et al.,

1982), and in the solar wind (Gurnett & Frank, 1978; Gurnett et al., 1979a; Kurth et al., 1979; Marsch et al., 1982).

Thus, in the next Section a detailed study of ion-beam instabilities with special emphasis in the ion-ion acoustic instability is presented.

III. ANALYTICAL APPROACH TO ION BEAM INSTABILITIES

Let us consider the electrostatic dispersion relation for waves propagating in a homogeneous plasma in the absence of the magnetic field:

$$1 = \sum_l \frac{w_{pe}^2}{k^2\,\alpha^2} \int d^3v\, [(\vec{k}\frac{\partial f_{0l}}{\partial \vec{v}}) / (w - \vec{k}.\vec{v})] \qquad (3)$$

The external magnetic field has been neglected because, as we have seen, Omidi (1985) has shown that the magnetic field has no effect on the BEN. The actual condition for neglecting the magnetic field was given by Gary (1970, 1971) who showed that the magnetic field can be neglected when $(k_{/\!/}\ \alpha_e/\Omega_e) > 4$. Such condition is easily met in the PSBL.

Assuming Maxwellian distribution functions for the electrons and the ion-core, and a drifting Maxwellian for the ion beam, eq. (3) yields:

$$1 = \frac{w_{pe}^2}{k^2\,\alpha^2}\, Z'\left(\frac{w}{k\alpha_e}\right) + \frac{w_{pi}^2}{k^2\,\alpha_i^2}\, Z'\left(\frac{w}{k\alpha_i}\right) +$$

$$+ \frac{w_{pb}^2}{k^2\,\alpha^2}\, Z'\left(\frac{w - k_{/\!/}U}{k\alpha_b}\right) \qquad (4)$$

This is a simple dispersion relation with the first term representing the electrons, the second the ion-core, and the third the ion-beam. Moreover, since in the PSBL $(w/k\alpha_e) << 1$, $(w/k\alpha_i) > 1$, and $(w - k_{/\!/}U)/k\alpha_b > 1$, we can use the power series expansion of the plasma dispersion function in the first term, and the asymptotic expansion in the other terms, to obtain the following:

$$y = -2\,[(U\cos\theta)/\alpha_e] + \frac{\delta\eta_b}{(1 - x/y)^2} + \frac{\delta\eta_i}{(x/y)^2} +$$

$$+ \frac{4\delta\eta_b\sqrt{\pi\gamma}}{y\, w_{pe}}\,[(U\cos\theta)/\alpha_e]^5\,(1 - x/y)^2\exp[-(1 - x/y)^2]\,[(U\cos\theta)/\alpha_b]^2$$

$$+ \frac{4\delta\eta_i\sqrt{\pi\gamma}}{y\, w_{pe}}\,[(U\cos\theta)/\alpha_i]^5\,(x/y)^2\exp\{-[(x\,U\cos\theta)/y\alpha_i]^2\} \qquad (5)$$

and

$$\gamma = \frac{w_{pe}\sqrt{\pi}\; x\,[(U\cos\theta/\alpha_e]^3\,F(x,y)}{\delta\eta_b/(1 - x/y)^2 - \delta\eta_i/(x/y)^2} \qquad (6)$$

where

$$F(x,y) = \exp\{-[(x\,U\cos\theta)/y\alpha_e]^2\} + \delta\eta_i\,(\alpha_e/\alpha_i)^2\exp[(x\,U\cos\theta)/y\alpha_i]^2$$

$$+ \delta\eta_b\,(\alpha_e/\alpha_b)^3\,(1 - y/x)\exp\{-[(1 - x/y)^2]\,[(U\cos\theta)/\alpha_i]^2\} \qquad (7)$$

$$\delta = \frac{m_e}{m_i}\,,\ \eta_b = \frac{n_b}{n_o}\,,\ \eta_i = \frac{n_i}{n_o}\,,\ x = w_r/w_{pe}\,,\ y = k_{/\!/}U/w_{pe}$$

Equations (5) and (6) constitute a system of algebraic coupled equations which are not very revealing. In the case of the ion-acoustic instability the last two terms in eq. (5) are negligible and the system becomes uncoupled. Nevertheless this is not so in the case of the ion-ion acoustic instability; therefore, the situation becomes more complex. However, we shall show that when the system of equations is complemented with the marginal instability condition, it provides a simple way to separate each one of the two unstable modes present in the system.

Notice that when the function F(x,y) is equal to zero, the growth rate given by eq. (6) is also zero. Consequently, the condition for marginal instability is F(x,y) = 0. Equations (5) and (6) are approximate equations obtained by using the asymptotic and power series expansion of the plasma dispersion function.

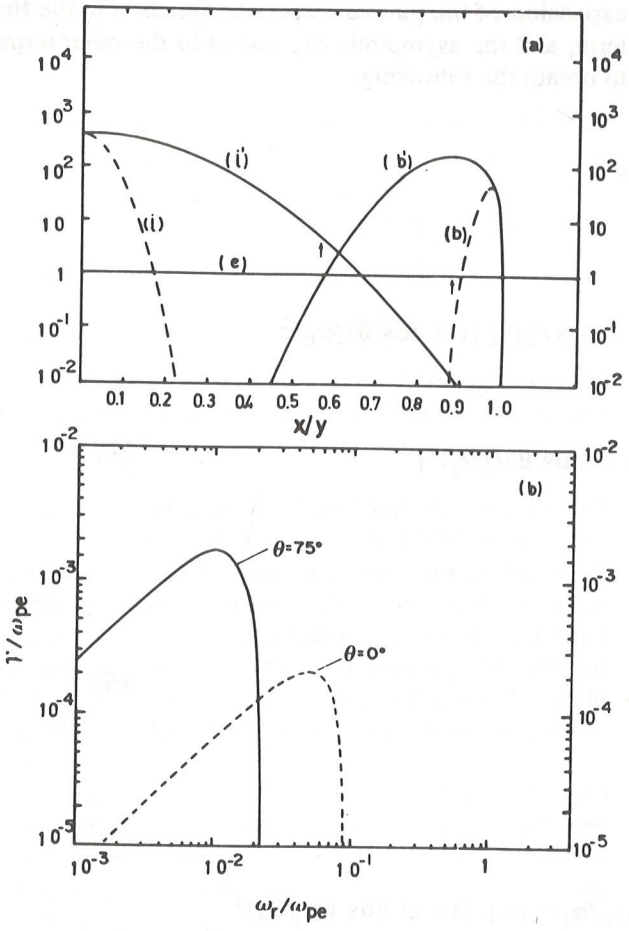

Figure 6. (a) The behaviour of each term in eq. 7 as a function of x/y. (b) Growth rate vs. frequency normalized to w_{pe}. The plasma parameters are $\eta_i = \eta_b = 0.5$, $U(\alpha_i) = 14.3$, $(U/\alpha_b) = 25$, $(U/\alpha_e) = 0.12$ for $\theta = 0^o$ (--) and $\theta = 75^o$ (-).

However, the condition for marginal instability is an exact relation which can be obtained by setting $\gamma = 0$ in eq. (4). Notice that eq. (7) is the sum of the exponential factors of the plasma dispersion function of each of the plasma components, and it can be equal to zero only if $y > x$. Otherwise, there are no solutions of the equation $F(x,y) = 0$. Thus, a necessary condition for instability is that the drift velocity should be larger than the parallel phase velocity.

Since the electrons in the PSBL satisfy $(w/k\alpha_e) << 1$, the first term in eq. (7) is of order one throughout the unstable frequency range. The behaviour of the ion-core term (i) and the ion-beam term (b) for $\theta = 0^o$ are shown in the upper panel of Fig. 6. The other curves (i') and (b') correspond to the same terms but for $\theta = 75^o$.

The condition for marginal instability is given by the intersection of curve (e) plus curve (i) with curve (b). We can see that at the point where the electron term (e) intersects the ion-beam term (b) the ion-core term is negligible. Due to the fact that the waves grow to the left of the intersection, the ion-core term will remain negligibly small as compared with the electronic term. We shall see that the unstable region never extends beyond (x/y) values less than 0.5, and therefore, it is clear that for parallel propagation the dominant instability is the one due to the relative drift between the ion-beam and the electrons, namely, the ion-acoustic instability.

As the propagation angle increases, the ion-core term and the ion-beam term open up in such a way that for $\theta = 75^o$ the intersection between the two terms occurs at a value which is about eight times larger than the electron term. Moreover, since the waves grow to the left of the intersections, the ion-core term becomes even larger. Therefore, the dominant instability now corresponds to the ion-ion acoustic instability which is due to the relative drift between the ion-core and the ion-beam.

The growth rate versus the real frequency, both normalized to the electron plasma frequency and calculated from eqs. (5) and (6), are shown in the lower panel of Fig. 6. We see that everything occurs as anticipated in very good agreement with the results of Omidi (1985). The arrows in the upper panel show the range of unstable frequencies for both instabilities. For the ion-acoustic instability, $x/y \simeq 0.9$, which implies that $w_r \simeq kU$. And, for the other instability, $x/y \simeq 0.55$, which means that the ion-ion acoustic instability grows in the regime $V_{p/\!/} \simeq U/2$.

From eqs. (5) and (6) we can see that the dependence on the drift velocity U and the propagation angle θ is always through the product $U \cos\theta$. This fact has immediate consequences on the behaviour of the growth rate of the instabilities.

In the case of the ion-ion acoustic instability, the aforementioned behaviour implies that an increase in

the drift velocity will produce a growth rate identical to the one shown in the lower panel of Fig. 6, but at a larger angle. Thus, increasing drift velocities lead to larger and larger angular thresholds of the ion-ion acoustic instability without changing either the maximum growth rate or the unstable frequency range. Notice that the angle can become very close to 90°, but it can never be equal to 90°. On the other hand, a reduction of the drift velocity decreases the angular threshold of the instability, in such a way that for sufficiently low drift velocities, the same growth rate with the same maximum value will occur at $\theta = 0^o$. Further reduction of the beam velocity will quench the instability. Thus, we conclude that the ion-ion acoustic instability can dominate over the ion-acoustic instability at any angle which value depends only on the drift velocity.

For the ion-acoustic instability, the dependence of the growth rate on the drift velocity and propagation angle implies that increasing drift velocities will lead to the same growth rate shown in Fig. 6 for $\theta = 0^o$, but now, for larger angles. However, since in this case the instability peaks at parallel propagation, the conclusion is now that increasing drift velocities enhance both the maximum growth rate and the high frequency cut off.

We shall demonstrate the same results from a different viewpoint, but now let us study the behaviour of the instabilities for decreasing beam temperatures.

The effect of decreasing beam temperatures is to shrink and increase the height of the beam term. In particular, for zero beam temperature the ion-beam term becomes a δ-function at (x/y) = 1.

In Fig. 7, we have taken the same plasma model of Fig. 6, but the beam temperature has been reduced by a factor of almost three. We have considered three propagation angles, $\theta = 0^o$, 60^o, 75^o. For $\theta = 0^o$, the ion-core term is negligible in the unstable frequency range and, therefore, the dominant instability is the ion-acoustic instability. For $\theta = 75^o$, at the intersection of the electron term and the ion-beam term, the ion-core term is one order of magnitude smaller than the other two terms. However, as we move into the instability region, the ion-core term becomes of the same order of the electron term and eventually overcomes this term. Therefore, in this case, the instability starts as a branch of the ion-acoustic instability, but as the instability grows, it suffers a transition to the ion-ion acoustic instability.

In the lower panel of Fig. 7 the corresponding growth rates are shown. As expected, the dominant mode for $\theta = 0^o$ and 60^o is the ion-acoustic instability. For $\theta = 75^o$ the transition from the ion-acoustic mode to the ion-ion acoustic mode is clearly seen. There is also a large enhancement of the unstable frequency range of both modes, and an important increase of the maximum growth rate of the ion-acoustic instability.

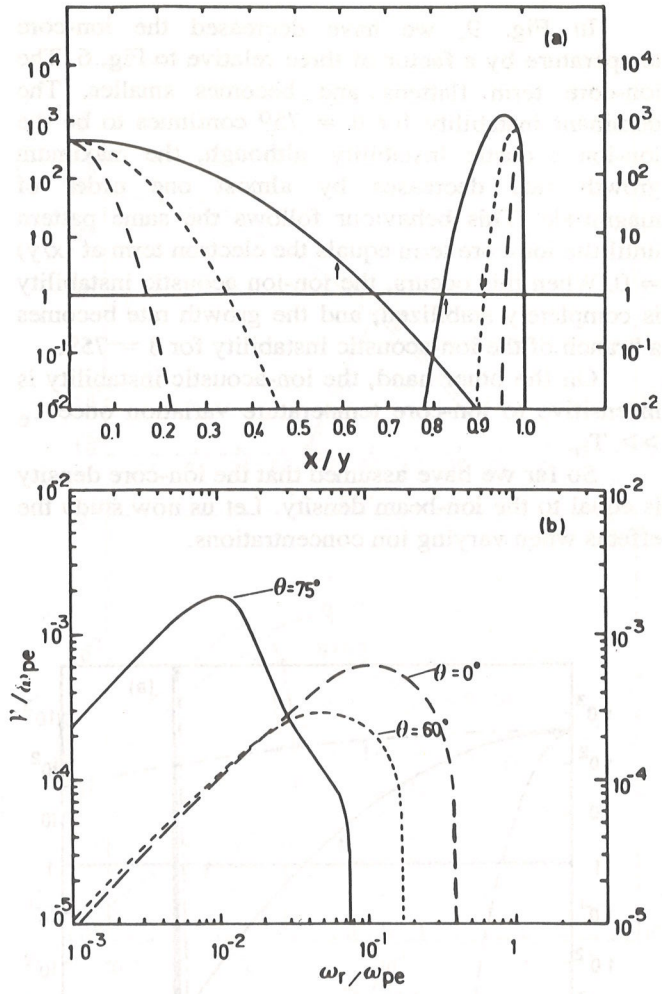

Figure 7. The same as Fig. 6 for a colder beam with $(U/\alpha_b) = 66.67$ and $\theta = 0^o$ (--), 60^o (...) and 75^o (-).

In Fig. 8, we have decreased the beam temperature by a factor of ten relative to Fig. 6. The δ function behaviour of the beam term is already clearly seen. In this case, we have considered $\theta = 0^o$, 75^o, 85^o. For $\theta = 0^o$, the dominant mode is the ion-acoustic instability. For $\theta = 75^o$, although at the intersection of the electron term and the ion-beam term, the ion-core term is now three orders of magnitude less than the electron term, we again expect to see a transition from one mode to the other. For $\theta = 85^o$, the ion-acoustic instability is negligible throughout the unstable frequency range. The corresponding growth rates are shown in the lower panel of Fig. 8. Everything occurs as expected: the ion-acoustic mode controlling the small angle propagation, a transition from one mode to the other at $\theta = 75^o$, and dominance of the ion-ion acoustic instability throughout at $\theta = 85^o$. It is interesting to notice that the high frequency cutoff is now larger than the electron plasma frequency. Furthermore the maximum growth rate of the ion-ion acoustic instability is almost insensitive to a decrease of the beam temperature, and it leads only to an increase of the angular threshold of the instability.

In Fig. 9, we have decreased the ion-core temperature by a factor of three relative to Fig. 6. The ion-core term flattens and becomes smaller. The dominant instability for $\theta = 75^o$ continues to be the ion-ion acoustic instability; although, the maximum growth rate decreases by almost one order of magnitude. This behaviour follows the same pattern until the ion-core term equals the electron term at (x/y) = 0. When this occurs, the ion-ion acoustic instability is completely stabilized, and the growth rate becomes a branch of the ion-acoustic instability for $\theta = 75^o$.

On the other hand, the ion-acoustic instability is insensitive to ion-core temperature variation once $T_e >> T_b$.

So far we have assumed that the ion-core density is equal to the ion-beam density. Let us now study the effects when varying ion concentrations.

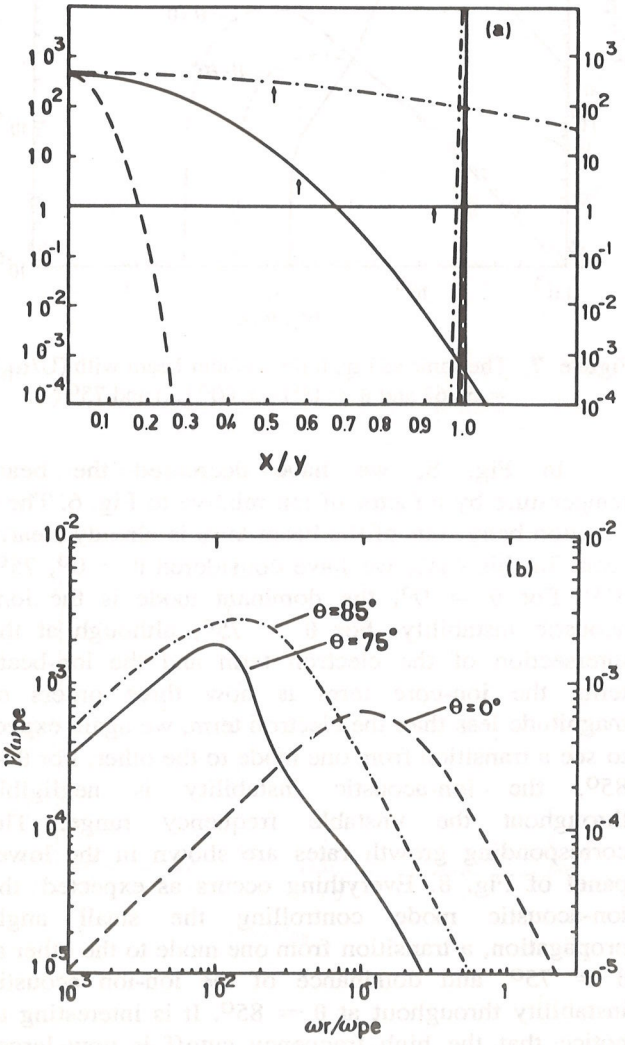

Figure 8. The same as Fig. 6 for a very cold beam with $(U/\alpha_b) = 2 \times 10^3$ for $\theta = 0^o$ (--), 75^o (-), and 85^o (--).

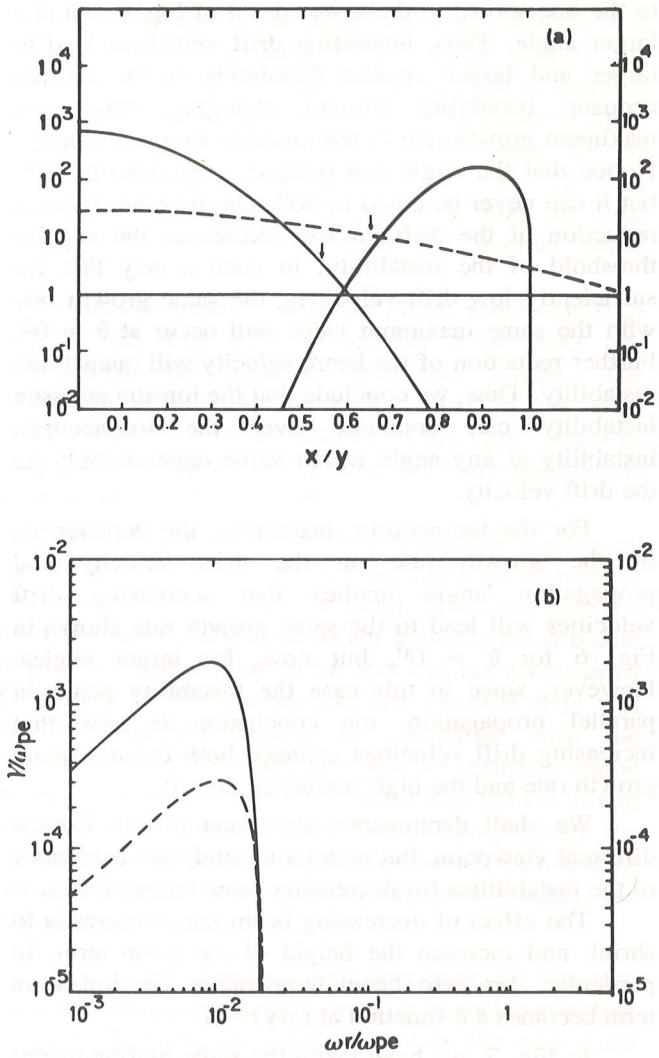

Figure 9. The same as Fig. 6 but for two ion-core temperatures, $(U/\alpha_i) = 16.67$ (-) and $(U/\alpha_i) = 5.9$ (--), for $\theta = 75^o$.

To this end, in Fig. 10 we start from the plasma model of Fig. 6 for $\theta = 75^o$, and reduce the ion-core density from $\eta_i = 0.5$ to $\eta_i = 0.01$. As shown in the figure, the intersection of the ion-core term and the ion-beam term goes down until it becomes less than one. Therefore, we expect that the maximum growth rate of the ion-ion acoustic instability will become smaller and smaller until the ion-acoustic mode will dominate. In the lower panel of Fig. 10, the behaviour of the growth rate is shown in terms of decreasing ion-core density. This decrease of the maximum growth rate is clearly seen. The curves which grow in the region of high frequencies correspond to parallel propagation, namely, the ion-acoustic mode. For $\theta = 75^o$ and $\eta_i = 0.01$ the growth rate has become a branch of the ion-acoustic mode in agreement with the behaviour anticipated in the upper panel of the figure.

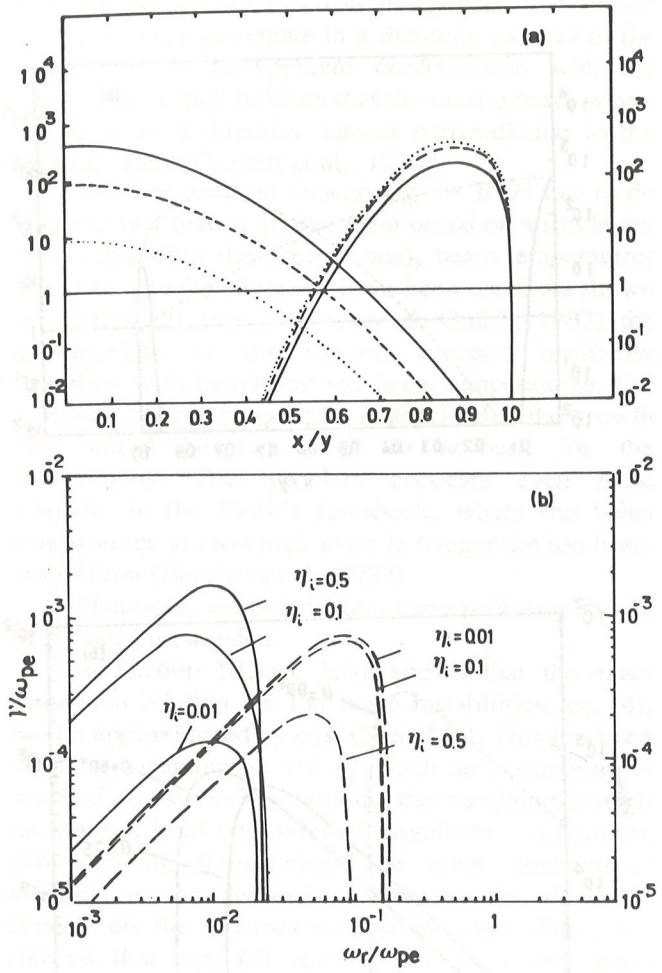

Figure 10. (a) The same as Fig. 6 but for varying ion-core densities; η_i = 0.5 (-), 0.1 (--), and 0.01 (---). The angle is θ = 75°. (b) Growth rates vs. frequency normalized to w_{pe} for θ = 0° (--) and 75° (-).

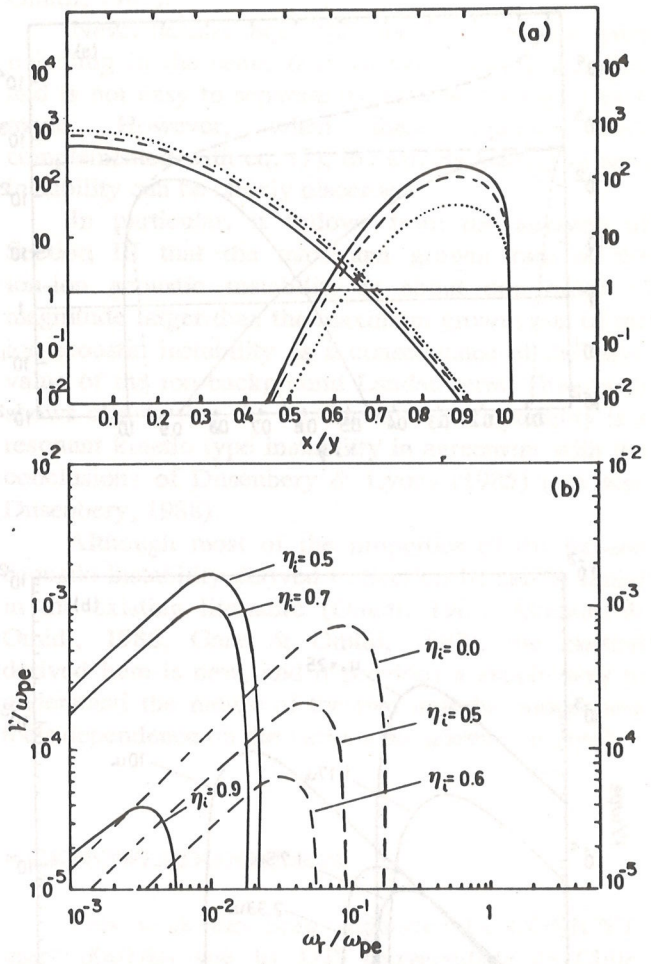

Figure 11. (a) The same as Fig. 10 but for η_i = 0.5 (-), 0.7 (--), and 0.9 (---). (b) Growth rates vs. frequency normalized to w_{pe}. For θ = 75° (-) η_i = 0.5, 0.7, 0.9 and for θ = 0° (--) η_i = 0.6, 0.5, and 0.

From eq. (7), we see that the ion-core term is multiplied by η_i, so that a decrease in η_i implies a constant shift downwards of the ion-core term. Likewise, an increase in the ion-core density implies a constant shift upwards of the ion-core term. The effect of increasing ion-core density is shown in Fig. 11. Despite the curve goes up as η_i increases beyond η_i = 0.5, the intersection of the beam term goes down, which implies that the maximum growth rate of the ion-ion acoustic instability decreases until it becomes again a branch of the ion-acoustic instability, as also seen in the previous figure. Thus, the conclusion is that as long as the ion-core is composed by the same type of ions that the ion-beam, the maximum growth rate of the ion-ion acoustic instability occurs for η_i = η_b = 0.5. The corresponding growth rates are shown in the lower panel of Fig. 11 together with the behaviour of the growth rate for parallel propagation.

Let us now go back to the effect of varying beam velocities. In Fig. 12, we consider the same plasma model of Fig. 6 for θ = 75°, where we have decreased the beam velocity by a factor of 10 (dashed line), and increased the beam velocity by a factor of 10 (dotted line). As the drift velocity decreases, the ion-core term flattens and the ion-beam term becomes wider and wider until it degenerates in the way indicated in the upper panel of the figure. When this situation is reached, both modes are damped since the ion-beam term is larger than the other two throughout the instability region.

When the drift velocity increases the ion-core and the ion-beam terms shrink leading thereby to a stabilization of the ion-ion acoustic instability. The ion-acoustic mode dominates even for θ = 75°. This result is explicitly illustrated in the lower panel of the figure, where the variation of the growth rate for θ = 75° in terms of increasing drift velocity is shown. The maximum growth rate decreases until the drift velocity becomes 1.75 U_o, and then starts increasing again as a branch of the ion-acoustic mode.

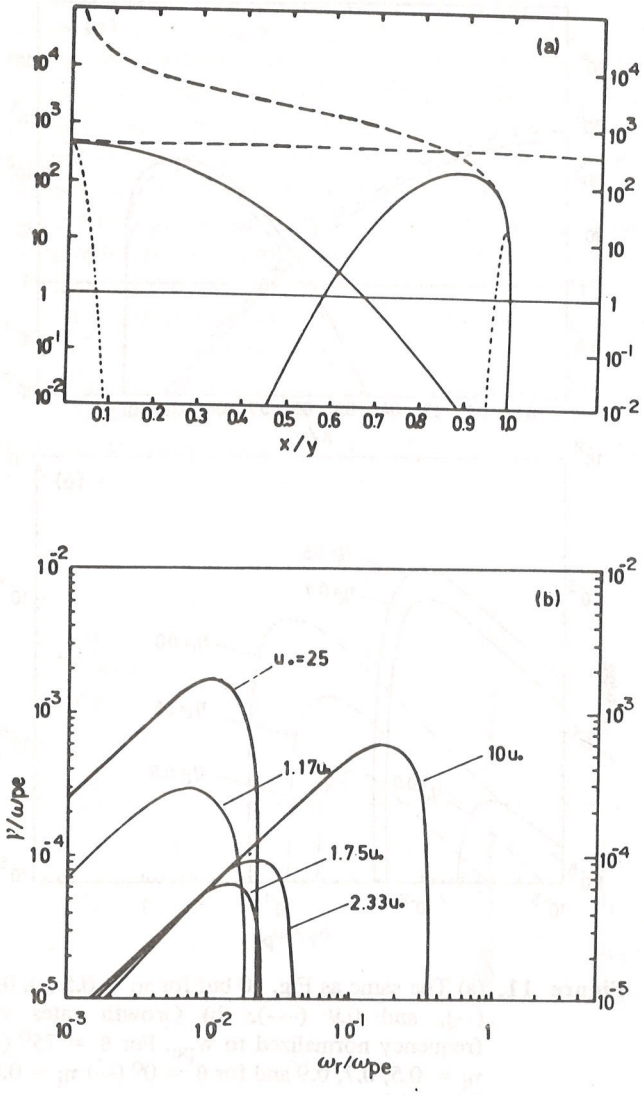

Figure 12. (a) The same as Fig. 6 for $\theta = 75^o$. The drift velocity has been increased (---) and reduced (--) by a factor of 10. (b) Growth rates for increasing drift velocities from $U_o = (U/\alpha_b) = 25$ to $(U/\alpha_b) = 10\ U_o$.

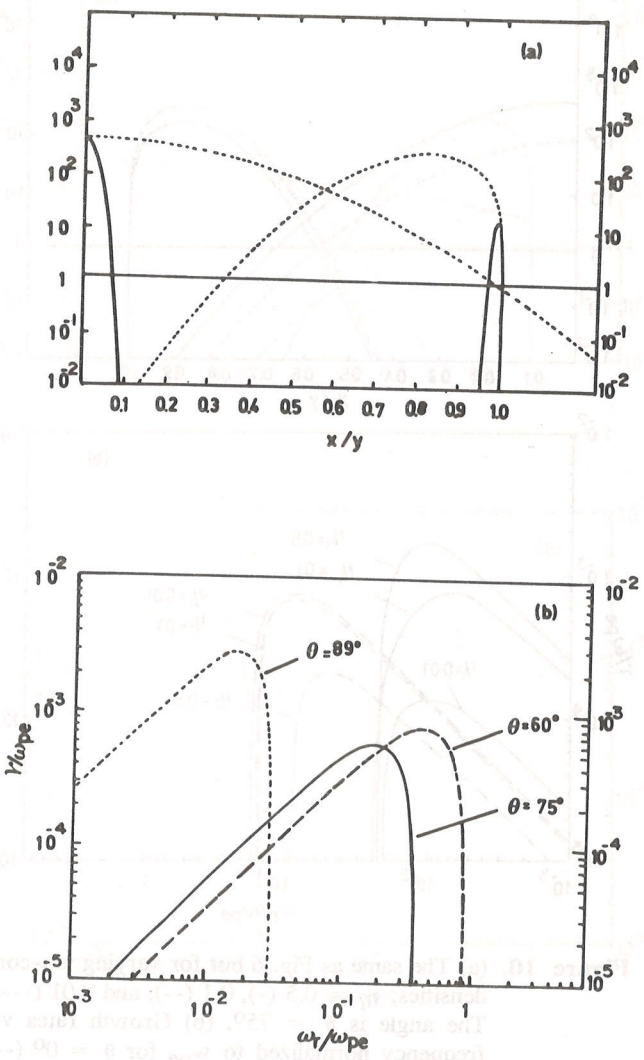

Figure 13. (a) The same as Fig. 6 for $(U/\alpha_b) = 250$ and $\theta = 75^o$ (-) and 89^o (---). (b) Growth rates for $\theta = 60^o$ (--), 75^o, and 85^o (---).

In Fig. 13, we start by considering the case when $U = 10\ U_o$ for $\theta = 75^o$ (full line) and increase the propagation angle to $\theta = 89^o$, to show that the ion-ion acoustic instability reappears at a very large angle. From the lower panel, we see that the ion-ion acoustic instability becomes indeed dominant, but at $\theta = 89^o$. Also, we can see that the growth rate for $\theta = 89^o$ is identical to the growth rate of Fig. 6 for $\theta = 75^o$. This is a consequence of the fact that the dependence on U, and θ is always through the product U cos θ, as explained previously.

IV. SUMMARY AND CONCLUSIONS

In Section II, we have seen that BEN can be understood in terms of a combination of instabilities with the low frequency region generated by the lower hybrid drift instability, and the high frequency region by ion beam instabilities.

However, the high frequency cutoff of the BEN extends up to w_{pe} and sometimes even beyond w_{pe}. This fact is difficult to understand, even when a minoritary cold electron component is assumed to exist

in the PSBL (Grabbe, 1987). Moreover, in the presence of a cold electron component, the fastest growing waves propagate in a direction parallel to the magnetic field in apparent contradiction with the observation which indicate that the most intense waves propagate in a direction almost perpendicular to the magnetic field (Gurnett et al., 1976).

Another problem concerning the BEN has to do with the fact that in all treatment based on a single ion beam (including the present one), beam temperatures less than actually observed have been used. As shown in Section III (see also Gary & Omidi, 1987) the growth rate of the ion-ion acoustic instability decreases with increasing ion beam temperatures. For observed beam temperatures in the PSBL, the growth rate would be too small to account for the observations. This problem becomes even more dramatic in the Earth's foreshock, where the beam temperatures are too high even to trigger the ion beam instabilities (Fuselier et al., 1987).

Therefore, we believe that these problems should be further investigated.

In Section III, we have shown that the exact dispersion relation for ion beam instabilities, eq. (4), can be approximated by eqs. (5) and (6). This has been done by assuming $\omega_r >> \gamma$. Such an assumption is justified a posteriori by noticing that maximum growth rates are at least one order of magnitude less than the corresponding frequencies. The other assumptions involved in the derivation of the analytical results depend on the external parameters used. Then, we showed that eqs. (5) and (6) are in a very good agreement with exact numerical results (Omidi, 1985; Akimoto & Omidi, 1986; Grabbe, 1987; Gary & Omidi, 1987).

Nevertheless, eqs. (5) and (6) are not very revealing in the sense that they describe two modes, and is not easy to separate the effects leading to each mode. However, when these equations are complemented with eq. (7), the effects leading to each instability can be clearly discerned.

In particular, it follows from the analysis of Section III that the maximum growth rate of the ion-ion acoustic instability is about one order of magnitude larger than the maximum growth rate of the ion-acoustic instability as a consequence of the large value of the ion-background Landau term. This result shows clearly that the ion-ion acoustic instability is a resonant kinetic type instability in agreement with the conclusions of Dusenbery & Lyons (1985) (see also Dusenbery, 1988).

Although most of the properties of the ion-ion acoustic instability derived in Section III can be found in the existing literature (Omidi, 1985; Akimoto & Omidi, 1986; Gary & Omidi, 1987), the method derived here is new, and it provides a simple way to understand the nature of the two unstable modes and their dependence on the various parameters involved.

ACKNOWLEDGEMENTS

This work has been supported by CONICYT, grant 0001/88 and by DTI Universidade de Chile, grant E2812/8812.

REFERENCES

AKIMOTO, K. & OMIDI, N. – 1986 – The generation of BEN by an ion beam in the magnetotail. Geophys. Res. Lett., 13: 97-100.

ANDERSON, R.R.; PARKS, G.K.; EASTMAN, T.E.; GURNETT, D.A. & FRANK, L.A. – 1981 – Plasma waves associated with energetic particles streaming into the solar wind from the earth's bow shock. J. Geophys. Res., 86: 4493-4510.

ASHOUR-ABDALLA, M. & THORNE, R.M. – 1977 – The importance of electrostatic ion cyclotron instability for quiet-time auroral precipitation. Geophys. Res. Lett., 4: 45-48.

CATTEL, C.A. & MOZER, F.S. – 1986 – Experimental determination of the dominant wave mode in the active near-earth magnetotail. Geophys. Res. Lett., 13: 221-224.

CATTEL, C.A.; MOZER, F.S.; HONES, E.W.; ANDERSON, R.R. & SHARP, D. – 1986 – ISEE observations of the plasma sheet boundary plasma sheet, and neutral sheet. 1. Electric field, magnetic field, plasma and ion composition. J. Geophys. Res., 91: 5663-5680.

DUSENBERY, P. – 1988 – Reply. J. Geophys. Res., 93: 14729-14731.

DUSENBERY, P. & LYONS, L. – 1985 – The generation of electrostatic noise in the plasma sheet boundary layer. J. Geophys. Res., 90: 10935-10943.

ETCHETO, J. & SAINT-MARC, A. – 1985 – Anomalous highly plasma densities in the plasma sheet boundary layer. J. Geophys. Res., 90: 5338-5344.

FORMISANO, V. & TORBERT, R. – 1982 – Ion acoustic wave forms generated by ion-ion streams at the earth's bow shock. Geophys. Res. Lett., 9: 207-210.

FORSLUND, D.W. & SHONK, C.R. – 1970 – Numerical simulation of electrostatic counterstreaming instabilities in ions beams. Phys. Rev. Lett., 25: 281-284.

FRIED, B. & CONTE, S. – 1961 – The plasma dispersion function. Academic Press, New York.

FUSELIER, J.A.; GARY, S.P.; THOMSEN, M.F.; BAME, S.J. & GURNETT, D.A. – 1987 – Ion beams and the ion-ion acoustic instability upstream from the earth's bow shock. J. Geophys. Res., 92: 4740-4744.

GALLAGHER, D.L. – 1985 – Short-wavelength electrostatic waves in the earth's magnetoheath. J. Geophys. Res., 90: 1435-1448.

GARY, S.P. – 1970 – Longitudinal waves in a perpendicular

collisionless plasma shock. II. Vlasov ions. J. Plasma Phys., **4**: 753-756.

GARY, S.P. – 1971 – ibid III, Te ~ Ti. J. Plasma Phys., **6**: 561.

GARY, S.P. & OMIDI, N. – 1987 – The ion-ion instability. J. Plasma Phys., **37**: 45-61.

GRABBE, C.L. – 1985 – New results on the generation of brodband electrostatic waves in the magnetotail. Geophys. Res. Lett., **12**: 487-490.

GRABBE, C.L. – 1987 – Numerical study of the spectrum of broadband electrostatic noise in the magnetotail. J. Geophys. Res., **92**: 1185-1192.

GRABBE, C.L. & EASTMAN, T.E. – 1984 – Generation of broadband electrostatic noise by ion beam instabilities in the magnetotail. J. Geophys. Res., **89**: 3865-3872.

GRESILLON, D.; DOVEIL, F. & BUZZI, J.M. – 1975 – Space correlation in ion-beam-plasma turbulence. Phys. Rev. Lett., **34**: 197-200.

GURNETT, D.A. & FRANK, L.A. – 1977 – A region of intense plasma wave turbulence on auroral field lines. J. Geophys. Res., **82**: 1031-1050.

GURNETT, D.A. & FRANK, L.A. – 1978 – Ion acoustic waves in the solar wind. J. Geophys. Res., **83**: 58-74.

GURNETT, D.A.; FRANK, L.A. & LEPPING, R.P. – 1976 – Plasma waves in the distant magnetotail. J. Geophys. Res., **81**: 6059-6071.

GURNETT, D.A.; KURTH, W.S. & SCARF, F.L. – 1981 – Plasma waves near Saturn: initial results from Voyager I. Science, **212**: 235-239.

GURNETT, D.A.; MARSCH, E.; PILIPP, W.; SCHWENN, R. & ROSENBAUER, H. – 1979a – Ion acoustic waves and related plasma observations in the solar wind. J. Geophys. Res., **84**: 2029-2038.

GURNETT, D.A.; NEUGEBAUER, F.M. & SCHWENN, R. – 1979b – Plasma wave turbulence associated with a interplanetary shock. J. Geophys. Res., **84**: 541-552.

HUBA, J.; GLADD, N. & PAPADOPOULUS, K. – 1978 – Lower-hybrid-drift wave turbulence at distant crossings of the plasma sheet boundaries and neutral sheet. Geophys. Res. Lett., **1**: 189-192.

KENNEL, C.F.; SCARF, F.L.; CORONITI, F.V.; SMITH, E.J. & GURNETT, D.A. – 1982 – Nonlocal plasma turbulence associated with interplanetary shocks. J. Geophys. Res., **87**: 17-34.

KURTH, W.S.; GURNETT, D.A. & SCARF, F.L. – 1979 – High-resolution spectrograms of ion acoustic waves in the solar wind. J. Geophys. Res., **84**: 3413-3419.

MARSCH, W., MUHLHAUSER, K.H., SCHWENN, R., ROSENBAUER, N., PILIPP, W. & NEUBAUER, F. – 1982 – Solar wind protons-3-dimensional velocity distributions and derived plasma parameters measured between 0.3 AU and 1-AU. J. Geophys. Res., **87**: 52-72.

MOSES, S.L.; CORONITI, F.V.; KENNEL, C.F.; SCARF, F.L.; GREENSTADT, E.W.; KURTH, H. & LEPPING, R.P. – 1985 – High time resolution plasma waves and magnetic field observations of the jovian bow shock. Geophys. Res. Lett., **12**: 183-186.

OMIDI, N. – 1985 – Broadband electrostatic noise produced by ion beams in the Earth's magnetotail. J. Geophys. Res., **90**: 12330-12334.

OMIDI, N. & AKIMOTO, K. – 1988 – Comment on "Generation of broadband noise in the magnetotail by beam acoustic instabilities". J. Geophys. Res., **93**: 14725-14728.

PASCHMANN, G.; SCKOPKE, N.; BAME, S.J. & GOSLING, J.T. – 1982 – Observation of gyrating ions in the foot of the nearly perpendicular bow shock. Geophys. Res. Lett., **9**: 881-884.

SCARF, F.; FRANK, L.; ACKERSON, K. & LEPPING, R. – 1974 – Plasma wave turbulence at distant crossings of the plasma sheet boundaries and neutral sheet. Geophys. Res. Lett., **1**: 189-192.

SCARF, F.L.; FREDERICKS, R.W.; FRANK, L.A.; RUSSELL, C.T.; COLEMAN, P.J. & NEUGEBAUER, M. – 1970 – Direct correlation of large-amplitude wave with suprathermal protons in the upstream solar wind. J. Geophys. Res., **75**: 7316-7322.

SCHRIVER, D. & ASHOUR-ABDALLA, M. – 1987 – Generation of high frequency broadband electrostatic noise: the role of cold electrons. J. Geophys. Res., **92**: 5807-5819.

THOMSEN, M.F. – 1985 – Collisionless schocks in the Heliosphere: reviews of current research (D.T. Tsurutani & R.G. Stone, ed.). Geophys. Monogr. Ser., **35**: 253.

Versão recebida em: 13/10/89
Versão revista e aceita em: 26/03/90
Editor Associado: V.W.J.H. Kirchhoff